

Evaluation of “Open Grid” protection strategy for a DC Network

S. Wang, R. Zheng*, J. Liang*, A. Adamczyk[†], C. D. Barker[†], R. S. Whitehouse[†]*

**Cardiff University, UK, WangS9@cf.ac.uk, [†]GE Grid Solution, UK, carl.barker1@ge.com*

Keywords: DC fault, HVDC Grid, protection, Open Grid

Abstract

“Open Grid” protection strategy is proposed for protecting DC networks with converters that cannot block fault current and rely on DC circuit breakers. With this method, each DC circuit breaker (DC-CB), based on its own, local measurements (e.g. overcurrent, undervoltage) trips without discrimination. Using the same local measurements, the DC-CBs, discriminate “healthy” DC circuit(s) and re-close. This mainly aims to increase the speed of fault current interruption and reduce the duty of an individual DC-CB in blocking a fault. This paper develops the protection algorithms which can meet DC protection requirement with different fault types, locations and fault impedances. The analysis of the fault behaviour following the action of protection system in the event of a DC fault has also been given. Different DC fault characteristics have been described. Further validations of the robustness of the Open Grid via simulation models developed in PSCAD/EMTDC have been provided. Tests have shown that the Open Grid can successfully detect and discriminate DC faults in a meshed DC grid model.

1 Introduction

The development of HVDC systems raises many research topics. Amongst those, one critical subject is the research on the protection of DC networks. Unlike faults that occur in an AC system where the propagation of fault current is limited by relatively large system inductance, the fault current rise and propagation in a DC system is much faster. Moreover, the system inductance only affects the rate of rise of the DC fault current, but not the current magnitude. Therefore, the anticipated speed of DC system protection acting to isolate a DC fault should be much faster than that of AC system protection. Consequently, protection algorithms have to be developed to detect a DC fault and interrupt the DC fault current within a very short time (e.g. 2-3ms [1]). A desirable outcome of this will be a lower fault current interruption requirement and a reducing in the energy dissipation requirements in DC-CBs.

There have been several methods of DC network protection proposed in [2-14]. Early stage work [2] presents a “handshaking method” within which DC fault currents can be extinguished by opening all AC circuit breakers (AC-CB) and the DC fault can then be isolated by fast DC switches. However, due to the delay caused by line energy dissipation

and relatively slow operation of AC circuit breakers, the fault isolation takes a long time (i.e. 0.5s) with this method. The protection algorithm in [3] detects faults based on measurement of current derivatives. This method is communication-dependent (i.e. current differential) to achieve fault detection and discrimination. However, long communication delays extend the operating time of the protection system. In [4], a protection strategy based on a combination of current and voltage wavelets is developed. It is claimed that the use of this strategy can be extremely fast to isolate and discriminate a fault. However, the signal processing delay of relays and data windows required for accurate analysis of wavelets are not considered. Reference [5] proposes a protection algorithm based on the measurement of differential voltage across inductors located on line ends. Note that differential voltage across a reactor is just current derivative by another means and it is described as not very capable to detect high impedance fault. References [6-7] propose methods based on travelling-waves. These methods may still not be capable of detecting faults with high impedance. References [8-9] also include the work on protection of offshore DC network for wind power integration. Recent work in [10] also presents a protection method using the measured rate of change of voltage to detect and discriminate a DC fault whilst with low fault impedance.

In the above protection methods, for locating faults and tripping DC-CBs, a certain delay is required to achieve discrimination. This increases the burden/stress on the DC-CBs. Alternatively, non-conventional DC network protection methods, have been proposed such as by GE’s Grid Solutions– Open Grid [11]. This method aims to further reduce the time for DC fault current interruption by changing the protection sequence order. By allowing each DC-CB to autonomously trip on detection of a fault without any delays associated with telecommunications or discrimination logics, the DC-CB opens at a much lower fault current.

In order to harness the apparent advantages of the Open Grid method, the challenges of developing the protection algorithm of fault detection and discrimination need to be addressed. To avoid any confusion, in the Open Grid concept, fault detection means the DC protection knowing there is a fault and thus DC-CBs can open without locating the fault. Fault discrimination means the DC protection determines the faulted section of the grid and guarantees the re-closure of DC-CBs to the healthy sections.

The first priority is to design an algorithm which can quickly detect a DC fault (e.g. <1ms). The second challenge is to

quickly determine which sections are healthy, so the associated DC-CBs can be reclosed if necessary. This paper addresses these challenges and contributes on the following items: 1. to develop and validate the algorithms for the detection and discrimination of faults; 2. to give analysis of the voltage and current profiles following the action of protection system.

2 Open Grid - (fault detection)

2.1 Basic idea of Open Grid

The core idea of the Open Grid is to change the protection sequence thus to block the fault current before spending time on discriminating or locating a DC fault (see Fig. 1 (a)). Multiple DC-CBs (may include some on healthy sections) simultaneously open to share of the fault current interruption duty based only on the measurements local to the breaker (e.g. overcurrent, undervoltage or even some combinations of current and voltage profiles). The fault current will then be interrupted with a much shorter time (and thus smaller magnitude) compared to using conventional method (see Fig. 1 (b)). This will bring down the current breaking requirements of DC protection devices and hence their cost. The protection system will then locate and discriminate the fault based on the measurable profiles such as residual DC voltages. The DC-CBs that are not located at the faulted section will re-close. Notice that the temporary open of more sections will not cause the interconnected AC system more disturbance since the discrimination will only take several milliseconds without any fault current. In fact, more sections being opened may spare some portion of the system from the voltage depression, comparing to the use of more conventional methods, which will take longer time to isolate the fault.

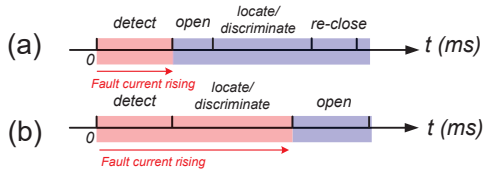


Fig. 1. Action order: (a) Open Grid; (b) conventional method.

2.2 Fault detection algorithm (open of DC-CBs)

When a low impedance fault occurs between the poles of a HVDC Grid, the DC voltage collapses and the fault current fed from the ac system, via the converters, increases rapidly (i.e. within a few milliseconds). As the fault propagating in a DC system is extremely fast, fault detection systems relying on communication systems will not be able to respond in time to prevent the fault currents reaching very high values. Therefore, the use of local time measurements of DC voltage (V_{dc}), DC current (I_{dc}), current direction and their derivatives ($\frac{dV_{dc}}{dt}$ and $\frac{dI_{dc}}{dt}$) at each DC-CB are the preferred signals for detection of DC fault.

An example of using local measurements to detect a DC fault

is given in Fig. 2 where a solid pole to pole fault is applied at the middle of one branch of a two-VSC, two-branch DC system. The system is rated at ± 200 kV and both branches are 200 km overhead lines (OHLs) which share the pre-fault current flowing from Bus B to Bus A. The DC-CBs (i.e. A1, A2, B1, and B2) are located at both ends of each branch. The DC-CBs are placed in series with reactors (e.g. 0.1 H) to limit the rate of rise of fault currents.

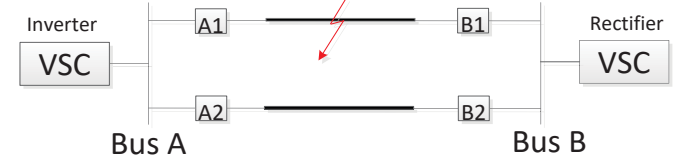


Fig. 2. One line diagram of the two-branch DC system.

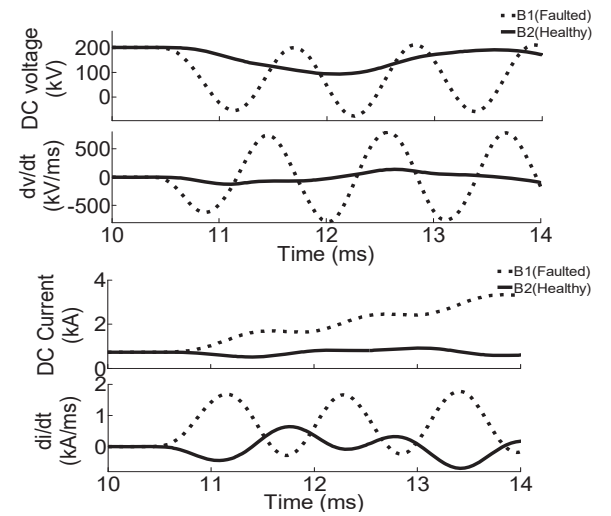


Fig. 3. Post-fault characteristics of voltage and current.

The fault occurs at the middle point of the circuit A1-B1 at 10 ms. Fig. 3 shows the voltages and currents which are measured at DC-CBs B1 (faulted) and B2 (healthy). Notice that, in this test, the DC-CBs remain closed and VSCs stay deblocked. It can be observed that the voltage wave front takes 0.5 ms to reach B1 and it temporarily oscillates to below zero within 0.6ms. However, the change of voltage at B2 is much smaller than at B1 due to the presence of the reactors associated with DC-CBs which separate these two measurement points. Meanwhile, the current at B1 doubles within 1ms after fault inception whilst the current direction of B2 tends to reverse to infed the faulted point.

Based on the above observations it would therefore appear reasonable to use voltage and current characteristics as the criteria for fault detection. A simple principle of fault detection is to use undervoltage, which allows a DC-CB to trip when the voltage drops below a voltage threshold (e.g. <150 kV). A similar approach can be made for current profile and the voltage and current derivatives to detect a fault.

2.3 Selection of criteria for fault detection

Amongst these four local measurements, the DC current flowing in the circuits can be very different. If the overcurrent

criterion is used for fault detection, the various loads of DC circuits could bring difficulty in setting of overcurrent thresholds in a highly meshed DC network. Moreover, the signal processing and actions of DC-CBs would cause more delay in waiting for the current to exceed the threshold. The DC-CBs may not be able to tolerate excessive current which is caused by the delay. However, the DC voltages at different points in the DC network are much more similar (assuming no DC/DC converters installed). The main difference in the DC voltage profile around the DC Grid is caused by current flowing through the resistances within the network. These differences are relatively minor and therefore, undervoltage is used as one criterion for fault detection.

However, if only undervoltage criterion is used (especially in a less capacitive network e.g. system connected by OHLs), DC-CBs may be incorrectly tripped in the event of AC system disturbance transferring onto the DC system which will lead to oscillations in the DC voltages. The robustness of detecting faults in the DC system may be improved by combining the undervoltage detection with other criteria such as the derivative of DC current (di/dt). Derivative signals by their very nature are “noisy” and to avoid spurious false triggering some form of filtering is required. In the example here, ten consecutive samples (sampling time was $20\mu s$ in this study) were used. The combination of criteria can then be expressed as:

$$\text{if } (|V_{dc}| < V_{thr}) \wedge \left(\left| \frac{di_{dc}}{dt} \right| > \frac{di}{dt}_{thr} \right) \text{ for ten consecutive samples,} \\ \text{then } flag_{fault} = 1 \quad (1)$$

It allows a DC-CB to start to trip off when ten consecutive data samples of voltages are lower than the pre-set thresholds and the current derivatives are larger than their thresholds.

3 Fault discrimination (residual voltage)

Following the isolation of the faulty circuit, the residual voltage on the healthy open circuit sections is used to identify the unfaulty circuits and the appropriate DC-CBs are reclosed. An example is given; Fig. 4 shows the residual voltages at DC-CBs B1 (faulted) and B2 (healthy) (see Fig. 2) following a solid pole to pole fault at the OHL connecting A1 and B1 at 10ms. Based on local measurements of DC voltage and current, the local protections open DC-CBs in both circuits. DC-CBs at A1 and B1 open at 11 ms followed by the opening of DC-CBs at A2 and B2 at 11.4 ms.

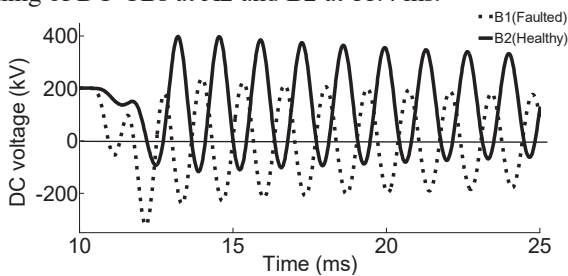


Fig. 4. Residual DC voltage after DC-CBs tripping.

In order to discriminate a faulted section from the healthy circuits, the difference between both voltage profiles should be highlighted. Both voltages are damping to different values and with different DC components. Therefore, potentially DC components of voltages are discriminative characteristics and methods of signal processing can be used to extract DC components from voltage oscillations. The observations of both DC voltages in Fig.4 show underdamped characteristics which can be expressed as:

$$V_{dc} = K_1 e^{-at} \cos(\omega_n t + \beta) + V_o \quad (2)$$

where K_1 is the magnitudes of first voltage oscillation, a is the decaying time constant, ω_n is the natural frequency of oscillation and V_o is the DC component. The parameter values in (2) for this example are shown in Table 1. These data are obtained using the Curve Fitting techniques.

Parameters	Faulted Circuit	Healthy Circuit
K_1	256.2 kV	285.5 kV
a	24.75	25.285
β	0	π
ω_n	$1483 \times \pi$ rad/s	$1483 \times \pi$ rad/s
V_o	0.04512 kV	131.6 kV

Table 1: Comparison of voltage profile.

The most discriminative factors are the DC components. The DC component of the faulted circuit is extremely close to zero whilst the healthy circuits retain a substantial and measurable DC component. Notice that in principle the DC component of the residual voltage at a pole to pole faulted circuit (*i.e.* short circuit) will theoretically be zero since the pre-fault energy charged in both poles of one symmetric DC circuit is balanced. A pole to ground fault will also cause the residual voltage on a faulted section to eventually collapse to zero due to the discharge of transmission line via the ground. However, the energy trapped within an opened healthy circuit cannot be discharged in a short term) and thus the DC component of its residual voltage will keep at a measurable level for a considerable period.

Therefore, the DC components of residual voltages are important indicators to discriminate a faulted circuit from a healthy circuit. The process of extraction of DC components can have slightly longer time than that of fault isolation since there is no fault current. This allows the use of integration based methods for the extraction including wavelet analysis and online Fast Fourier Transfer (FFT) with moving data windows. Due to inherent characteristics of OHLs and cables, when certain lengths are known (e.g. natural frequency), it is possible to determine initial size of data windows and base frequency. This will save time for frequency tracking thus further speeding up the online adjustment of data windows and the fault discrimination process.

Fig.5 shows the extracted DC components of voltages given in Fig.4 using online FFT. The DC component of voltage on the faulted circuit drops to zero while that on the healthy

circuit is at 131.6 kV which matches the curve fitting result in Table I. By giving a threshold between them (e.g. $V_o > 50$ kV within a moving data window of 3ms) the protection system can discriminate the faulted section and enable the re-closure of DC-CBs on healthy circuits.

The robustness of using residual voltages for discrimination is guaranteed by fast opening DC-CBs which traps energy within opened healthy circuits and keeps DC component of voltages at a non-zero level. The drawback of only using residual voltages is that, to extract a reasonably accurate measurement of the dc component requires integration over one cycle of the oscillation frequency (which is line length dependent). Delay is thus still required to make the decision of discrimination. In some events of fault where the margin between the voltages at the faulted section and the healthy section may be small, slightly longer delays may be needed to get a stable DC component and thus to achieve discrimination. This is further discussed in Section 4.

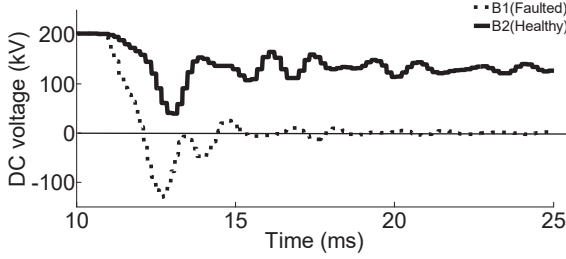


Fig. 5. Extracted DC component of residual DC voltage.

4 Fault discrimination (transient current)

The DC components of residual voltage on opened healthy circuits are determined by the energy trapped within them. At the time the DC-CBs open, current flow has ceased and the energy is transferred as a charge (and hence voltage) on the transmission line capacitance. Moreover, this trapped energy is also related to parameters of the transmission line and the energy stored in the line capacitance. This brings uncertainty of the DC components of voltage at healthy circuits. However, as previously mentioned, if the DC-CBs open within reasonable time, it is very unlikely that the energy trapped within opened healthy circuits is zero which further indicates a zero voltage. The least discriminative situations could be very high impedance pole to ground faults occurring at the symmetric monopole system. As the DC side of such a topology is not fed by its ac side current [12], there will only be a transient fault current as the fault is applied. Furthermore the large impedance will make the speed of discharge of a faulted section and healthy sections similar and hence discrimination more problematic. Conventional methods including current differential [13] are potential solutions to detect and discriminate a high impedance pole to ground fault. However such solutions will require a relatively long operating time.

Alternatively, within the Open Grid methodology, the discrimination can be achieved using the integration of pre-tripping transient current. An example is given in Fig. 6. A very high impedance fault of 400 ohms is applied at the same position as the previous test. The DC-CBs are tripped-off based on the same tripping logic. DC-CB at B1 opens at 11.2ms and B2 opens at 11.7ms. It can be observed that the extracted DC components of healthy circuits are 31.19 kV. The use of small threshold of residual voltage for discriminating in such a fault event (e.g. >20 kV). However, a larger delay could be used to obtain a stable dc component of the DC voltage at the faulted circuit since the margin of both dc components is small.

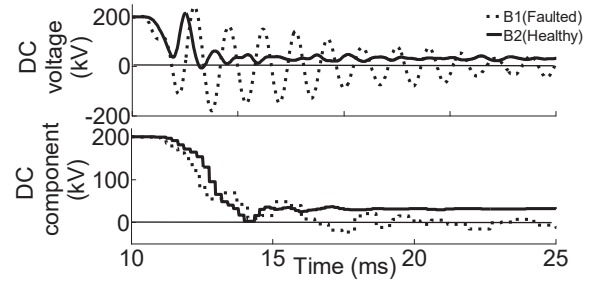


Fig. 6. residual voltage (a) measurement; (b) dc component.

In order to guarantee successful discrimination while further increasing its speed, criterion of integration of pre-tripping transient current (also known as electric charge) can be added, combining with the use of residual voltage. Fig.7 shows the sign of the integration of pre-tripping transient current on faulted circuits (represented by Q_{A1} and Q_{B1}). It indicates that at both line ends, the transient current over time will flow internally into the section to feed the fault. Meanwhile, for healthy circuits with voltage decreasing (See Fig.8 (a)), the DC-CBs of at least one line end, must have an integration of current tending to flow to the external during transient time. In some events (See Fig.8 (b)), the current may even tend to flow outside from both line ends due to the fast discharge of capacitive component close to line ends of either an OHL or a DC cable. Therefore, from at least one end of a healthy circuit, the integration of transient current will tend to flow out before the DC-CBs tripping off. This characteristic can be used as another criterion for fast discrimination as expressed below:

$$\text{if } Q_m = \int_{T-\Delta t1}^T \left(\frac{di}{dt} \right) dt > Q_{thr}; \text{ then } flag_{fault} = 0 \quad (3)$$

where the time T is the moment that a fault flag turned on which firstly opens the low voltage switch (given as PE1 in Fig. 9) of a hybrid DC-CB. $\Delta t1$ is the size of a window for integrating. The threshold can be set to zero as a critical point for the sign of integrated current reverses. If the integrated current flowing out from both ends of a section (as shown in Fig. 8 (b)), the DC-CBs can re-close the low voltage switch directly irrespective to its measured residual DC voltage and thus the discrimination is achieved. Notice that since the commutation branch (PE2) is still conducting, the currents are

not interrupted. For the healthy circuit with integrated current flowing outside at only one end, the local relay of the DC-CB can generate a re-close flag by (3) and the local DC-CB will stop opening. This allows the section to be charged through one line end, which further leads to the re-closure of remote DC-CB as this will obviously exceed the residual voltage detection level. Meanwhile, if telecommunication is available, the re-close flag can also be sent to the remote end of circuit via telecommunication to guarantee the discrimination. Notice that since the fault is isolated, there is no fault current circulating and thus the delay of telecommunication (e.g. 12 ms) is much less critical. The advantage of using this integration of pre-tripping transient current criterion allows the thresholds of residual voltage criterion to be set to a higher value. Moreover, compared to other proposed protection methods such as current differential algorithm, there is no need for synchronising the signals of both ends. The action of one DC-CB throughout an event of DC fault is summarised as Fig. 10.

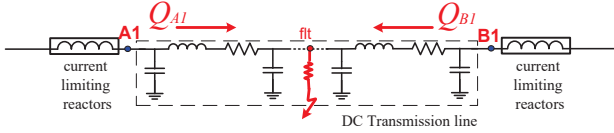


Fig. 7. Integration of transient current (faulted circuit).

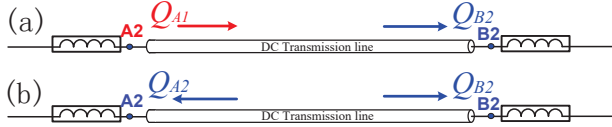


Fig. 8. Integration of transient current (healthy circuit).

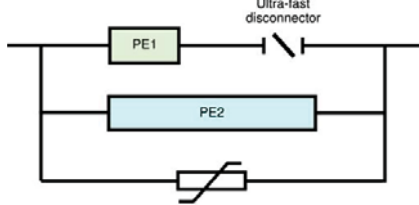


Fig. 9. Basic concept of a hybrid DC circuit breaker.

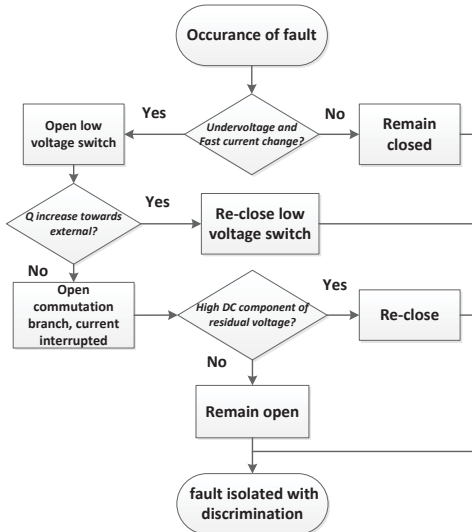


Fig. 10. Flow chart of DC-CB acting in a fault event.

5 Simulation study

5.1 Tested system

The protection algorithm is tested on a 4-converter, symmetric monopole DC system rated at ± 200 kV. This system is meshed by three OHLs and one cable (See Fig. 11). DC-CBs are located at both ends of each DC line. The entire system is high impedance grounded at its DC side. Converters VSC1 and VSC2 are under the alternative DC voltage droop control [14] while converters VSC3 and VSC4 are in the power control mode. The modelling of each component is introduced in [15].

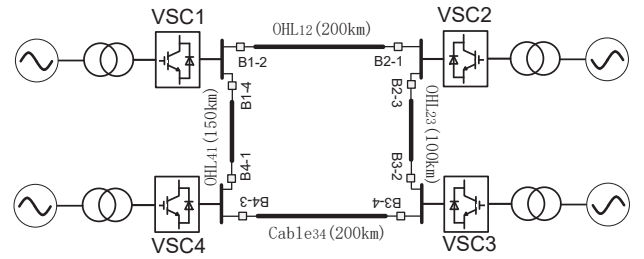


Fig. 11. One line diagram of meshed DC test system.

5.2 Case Study

A solid pole to pole fault is applied at the middle point of OHL12 at 10ms. Fig 12 (a) and Fig. 12(b) show the voltage and current profiles of positive pole. The voltage and current profiles of the negative pole are symmetric to the positive pole for a pole to pole fault (i.e. same magnitude but different signs) and thus are not given. The fault is isolated within 0.85 ms when DC-CBs at both ends of faulted section open (see Fig. 12 (c)). The fault current is thus interrupted fast and limited to 1.5p.u. Thereafter, the discrimination is achieved within 7ms when the DC-CBs on the healthy circuit all re-close. Fig. 13 (a) to Fig. 13 (c) shows the diagrams of integrations of transient current and current derivatives. Since the fault occurs at the middle of OHL12, the currents at B1-2 and B2-1 tend to infeed the faulted point at the same time. The integrations of transient currents before DC-CBs opening are thus positive at both ends. Meanwhile, DC-CBs at OHL23 and OHL41 also generate open signals by detecting undervoltages and fast change of currents. B4-1 and B2-3 are then temporary opened also since the integrations of transient currents at these two points are positive. B1-4 and B3-2 however immediately receive re-close signals by obtaining negative integrations of transient currents and thus stop opening. Fig. 14(a) to Fig. 14 (b) shows the zoomed in voltages and their extracted DC components. The DC components of voltages at faulted section equals to zero and B1-2, B2-1 remain open. The discrimination is achieved when B3-2 and B4-1 re-close based on high DC components of residual voltages (i.e. >50 kV) within the data window.

The benefits of using Open Grid are demonstrated by the extremely fast opening of DC-CBs and the fault current is limited to 1.5p.u. This brings down the rating of current interruption of the DC-CBs.

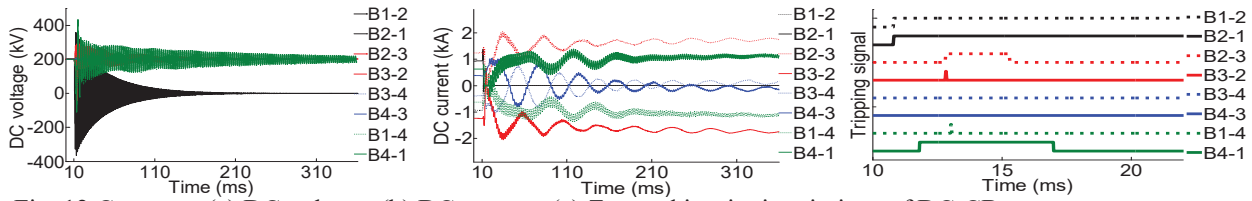


Fig. 12 Case one: (a) DC voltage; (b) DC current; (c) Zoomed in tripping timings of DC-CBs.

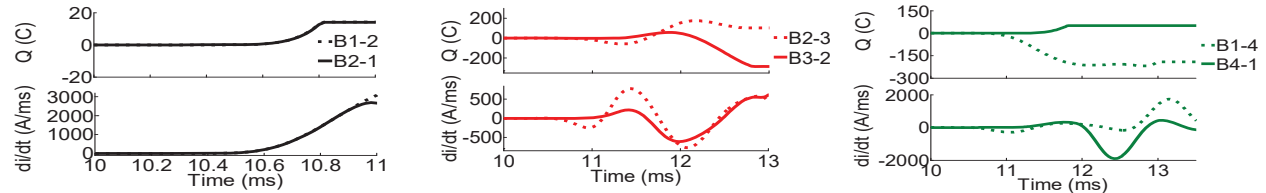


Fig. 13 Integration of current and derivatives obtained by DC-CBs at: (a) OHL12; (b) OHL23; (c) OHL14.

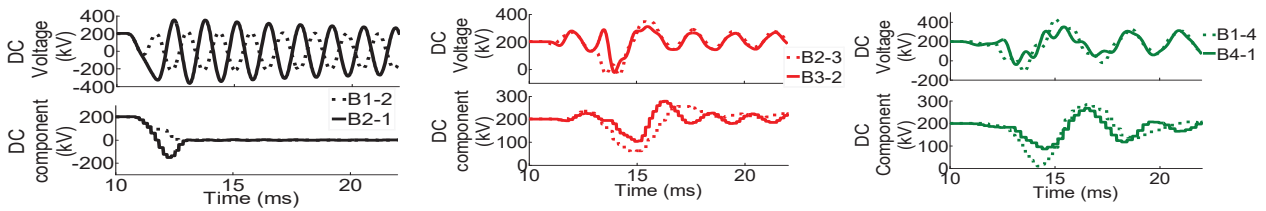


Fig. 14 Zoomed in DC voltages and their DC components at (a): OHL12; (b) OHL23; (c) OHL14.

6 Conclusion

The speed of DC network protection is of great importance. This paper shows the feasibility of using Open Grid within which DC-CBs trip rapidly based on local measurements to isolate the fault and then achieve discrimination afterwards. This change of protection sequence avoids the delay caused by discrimination for isolating a fault and thus reduces the time for fault current interruption. The interruption of smaller fault current may further bring down the size of protection devices (e.g. reactors of DC-CBs).

References

- [1] S., Athula and D. Rajapakse, "DC Fault Protection of a Nine-terminal MMC HVDC Grid", in *11th IET Int. Conf. AC DC Power Transm.*, Birmingham, 2015.
- [2] L.Tang and B.T. Ooi, "Locating And Isolating DC Faults in Multi-terminal DC Systems," *IEEE Trans. Power Del.*, vol.22, no.3, pp.1877-1884, July 2007.
- [3] A. Adamczyk, C.D. Barker and H. Ha, "Fault Detection and Branch Identification for HVDC Grids," in *12th IET Int. Conf. Develop. Power Syst. Protect.*, pp.1-6, 2014.
- [4] K. D. Kerf, et al., "Wavelet-based Protection Strategy for DC Faults in MTDC systems," *IET Gener. Transmiss. Distrib.*, vol.5, no.4, pp.496-503, 2011.
- [5] R. Li, L. Xu and L.Yao "DC Fault Detection And Location in Meshed Multiterminal hvdc Systems Based on DC Reactor Voltage Change Rate", *IEEE Trans. Power Del.* vol. 32, no. 3, 2017.
- [6] Y. Zhang, N. Tai and B. Xu, "Fault Analysis And Traveling-wave Protection Scheme for Bipolar HVDC Lines," *IEEE Trans. Power Del.*, vol.27, no.3, pp.1583-1591, July 2012.
- [7] J. Cheng, et al., "Paralleled Multi-terminal DC Transmission Line Fault Locating Method Based on Travelling Wave," *IET Gener. Transmiss. Distrib.*, vol. 8, no. 12, pp. 2092-2101, Dec. 2014.
- [8] Y. Jin, J. E. Fletcher, and J.O. Reilly. "Multiterminal DC Wind Farm Collection Grid Internal Fault Analysis And Protection Design." *IEEE Trans. Power Del.*, vol. 25, no.4, pp 2308-2318, 2010.
- [9] D. Jovcic, M. Taherbaneh, J.P. Taisne and S. Nguefeu, "Topology Assessment for 3+3 terminal Offshore DC Grid Considering DC Fault Management," *IET Gener. Transmiss. Distrib.*, vol. 9, no. 3, pp. 221-230, 2015
- [10] J. Sneath and A.D. Rajapakse., "Fault Detection and Interruption in An Earthed HVDC Grid Using ROCOV and Hybrid DC Breakers," *IEEE Trans. Power Del.*, vol. 31, no. 3, 2016.
- [11] C.D. Barker, R.S. Whitehouse, "An Alternative Approach to HVDC Grid Protection," in *10th IET Int. Conf. ACDC Power Transm. (ACDC)* pp.1-6, Dec. 2012.
- [12] E. Kontos, R.T. Pinto, S. Rodrigues, and P. Bauer, "Impact of HVDC Transmission System Topology on Multi-terminal dc Network Faults," *IEEE Trans. Power Del.* vol. 30, no. 2, pp. 844-852, April 2015.
- [13] J. Descloux, et al, "HVDC Meshed Grid: Control And Protection of A Multi-terminal HVDC System," in *Proc. Cigre Conf.*, France, 2012.
- [14] S. Wang, C. D. Barker, R. S. Whitehouse and J. Liang, "Experimental Validation of Autonomous Converter Control in a HVDC Grid", in *Proc. Eur. Conf. Power Electron. Appl.*, 2014, pp. 1–10.
- [15] S. Wang, et al., "Coordination of MMCS with Hybrid DC Circuit Breakers for HVDC Grid Protection" *IEEE Trans. Power Del.*, 2018 (early access).